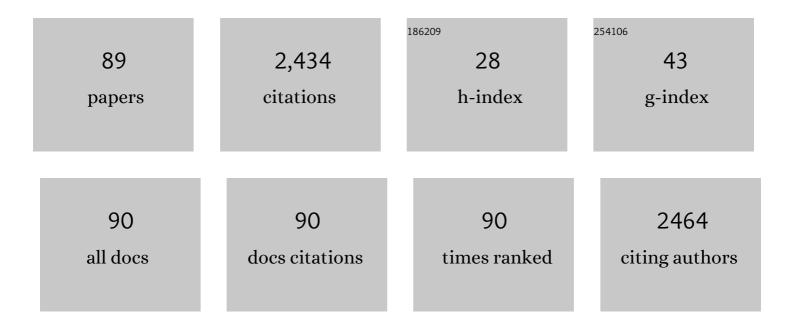
List of Publications by Year in descending order

Source: https://exaly.com/author-pdf/8276662/publications.pdf Version: 2024-02-01



#	Article	IF	CITATIONS
1	Single-atom Cu anchored catalysts for photocatalytic renewable H2 production with a quantum efficiency of 56%. Nature Communications, 2022, 13, 58.	5.8	175
2	Covalent organic framework-supported Fe–TiO ₂ nanoparticles as ambient-light-active photocatalysts. Journal of Materials Chemistry A, 2019, 7, 16364-16371.	5.2	103
3	A Metal–Organic Compound as Cathode Material with Superhigh Capacity Achieved by Reversible Cationic and Anionic Redox Chemistry for Highâ€Energy Sodiumâ€Ion Batteries. Angewandte Chemie - International Edition, 2017, 56, 6793-6797.	7.2	85
4	Platinum-Supported Cerium-Doped Indium Oxide for Highly Sensitive Triethylamine Gas Sensing with Good Antihumidity. ACS Applied Materials & Interfaces, 2020, 12, 42962-42970.	4.0	78
5	Synergistic Effect of the Surface Vacancy Defects for Promoting Photocatalytic Stability and Activity of ZnS Nanoparticles. ACS Catalysis, 2021, 11, 13255-13265.	5.5	71
6	Facile lotus-leaf-templated synthesis and enhanced xylene gas sensing properties of Ag-LaFeO ₃ nanoparticles. Journal of Materials Chemistry C, 2018, 6, 6138-6145.	2.7	70
7	Single-atom silver loaded on tungsten oxide with oxygen vacancies for high performance triethylamine gas sensors. Journal of Materials Chemistry A, 2021, 9, 8704-8710.	5.2	69
8	Formaldehyde sensing performance of reduced graphene oxide-wrapped hollow SnO2 nanospheres composites. Sensors and Actuators B: Chemical, 2020, 307, 127584.	4.0	57
9	Boron-doped graphene quantum dot/Ag–LaFeO ₃ p–p heterojunctions for sensitive and selective benzene detection. Journal of Materials Chemistry A, 2018, 6, 12647-12653.	5.2	51
10	Mesopore-rich carbon flakes derived from lotus leaves and it's ultrahigh performance for supercapacitors. Electrochimica Acta, 2020, 333, 135481.	2.6	51
11	Gas sensing materials roadmap. Journal of Physics Condensed Matter, 2021, 33, 303001.	0.7	49
12	Designed Highly Effective Photocatalyst of Anatase TiO2 Codoped with Nitrogen and Vanadium Under Visible-light Irradiation Using First-principles. Catalysis Letters, 2008, 124, 111-117.	1.4	47
13	A gas sensor array for the simultaneous detection of multiple VOCs. Scientific Reports, 2017, 7, 1960.	1.6	46
14	Single atom catalyst for electrocatalysis. Chinese Chemical Letters, 2021, 32, 2947-2962.	4.8	43
15	Highly selective and sensitive methanol gas sensor based on molecular imprinted silver-doped LaFeO ₃ core–shell and cage structures. Nanotechnology, 2018, 29, 145503.	1.3	42
16	B, N, S, Cl doped graphene quantum dots and their effects on gas-sensing properties of Ag-LaFeO3. Sensors and Actuators B: Chemical, 2018, 266, 364-374.	4.0	41
17	Boosted Visible-Light Photodegradation of Methylene Blue by V and Co Co-Doped TiO2. Materials, 2018, 11, 1946.	1.3	41
18	A highly sensitive and selective formaldehyde gas sensor using a molecular imprinting technique based on Ag–LaFeO ₃ . Journal of Materials Chemistry C, 2014, 2, 10067-10072.	2.7	39

#	Article	IF	CITATIONS
19	Band Alignment Strategy for Printable Triple Mesoscopic Perovskite Solar Cells with Enhanced Photovoltage. ACS Applied Energy Materials, 2019, 2, 2034-2042.	2.5	38
20	A Metal–Organic Compound as Cathode Material with Superhigh Capacity Achieved by Reversible Cationic and Anionic Redox Chemistry for Highâ€Energy Sodiumâ€Ion Batteries. Angewandte Chemie, 2017, 129, 6897-6901.	1.6	36
21	High selectivity methanol sensor based on Co-Fe2O3/ SmFeO3 p-n heterojunction composites. Journal of Alloys and Compounds, 2018, 765, 193-200.	2.8	36
22	Rich oxygen vacancies, mesoporous TiO ₂ derived from MIL-125 for highly efficient photocatalytic hydrogen evolution. Chemical Communications, 2021, 57, 9704-9707.	2.2	36
23	Pt Single Atom-Induced Activation Energy and Adsorption Enhancement for an Ultrasensitive ppb-Level Methanol Gas Sensor. ACS Sensors, 2022, 7, 199-206.	4.0	36
24	Efficient Compact-Layer-Free, Hole-Conductor-Free, Fully Printable Mesoscopic Perovskite Solar Cell. Journal of Physical Chemistry Letters, 2016, 7, 4142-4146.	2.1	35
25	Gas Sensors Based on Molecular Imprinting Technology. Sensors, 2017, 17, 1567.	2.1	35
26	Ag Nanoparticles Sensitized In2O3 Nanograin for the Ultrasensitive HCHO Detection at Room Temperature. Nanoscale Research Letters, 2019, 14, 365.	3.1	34
27	Inâ€Situâ€Formed Hierarchical Metal–Organic Flexible Cathode for Highâ€Energy Sodiumâ€Ion Batteries. ChemSusChem, 2017, 10, 4704-4708.	3.6	33
28	Raspberry-like mesoporous Co-doped TiO ₂ nanospheres for a high-performance formaldehyde gas sensor. Journal of Materials Chemistry A, 2021, 9, 6529-6537.	5.2	33
29	Advances of the functionalized carbon nitrides for electrocatalysis. , 2022, 4, 211-236.		33
30	Interface Engineering Based on Liquid Metal for Compact-Layer-free, Fully Printable Mesoscopic Perovskite Solar Cells. ACS Applied Materials & Interfaces, 2018, 10, 15616-15623.	4.0	31
31	A high selective methanol gas sensor based on molecular imprinted Ag-LaFeO3 fibers. Scientific Reports, 2017, 7, 12110.	1.6	30
32	Ag-LaFeO3/NCQDs p-n heterojunctions for superior methanol gas sensing performance. Materials Research Bulletin, 2019, 115, 55-64.	2.7	30
33	Excellent toluene gas sensing properties of molecular imprinted Ag-LaFeO3 nanostructures synthesized by microwave-assisted process. Materials Research Bulletin, 2019, 111, 320-328.	2.7	30
34	DFT calculations for single-atom confinement effects of noble metals on monolayer g-C ₃ N ₄ for photocatalytic applications. RSC Advances, 2021, 11, 4276-4285.	1.7	29
35	Regulating effect on photocatalytic water splitting performance of g-C3N4 via confinement of single atom Pt based on energy band engineering: A first principles investigation. Applied Surface Science, 2022, 577, 151916.	3.1	28
36	Efficient hole-conductor-free printable mesoscopic perovskite solar cells based on SnO2 compact layer. Electrochimica Acta, 2018, 263, 134-139.	2.6	27

#	Article	IF	CITATIONS
37	Formaldehyde gas sensor with extremely high response employing cobalt-doped SnO ₂ ultrafine nanoparticles. Nanoscale Advances, 2022, 4, 824-836.	2.2	27
38	Ag–LaFeO ₃ fibers, spheres, and cages for ultrasensitive detection of formaldehyde at low operating temperatures. Physical Chemistry Chemical Physics, 2017, 19, 6973-6980.	1.3	26
39	Sustainable cycling enabled by a high-concentration electrolyte for lithium-organic batteries. Chemical Communications, 2019, 55, 608-611.	2.2	26
40	Ultrasensitive xylene gas sensor based on flower-like SnO ₂ /Co ₃ O ₄ nanorods composites prepared by facile two-step synthesis method. Nanotechnology, 2020, 31, 255501.	1.3	26
41	Nearâ€Roomâ€Temperature Ethanol Gas Sensor Based on Mesoporous Ag/Zn–LaFeO ₃ Nanocomposite. Advanced Materials Interfaces, 2019, 6, 1801453.	1.9	25
42	Molecular imprinting Ag-LaFeO3 spheres for highly sensitive acetone gas detection. Materials Research Bulletin, 2019, 109, 265-272.	2.7	24
43	Synergistic Effects of Sm and C Co-Doped Mixed Phase Crystalline TiO2 for Visible Light Photocatalytic Activity. Materials, 2017, 10, 209.	1.3	23
44	Design of hollow dodecahedral Cu2O nanocages for ethanol gas sensing. Materials Letters, 2019, 247, 15-18.	1.3	23
45	Analysis of sulfur modification mechanism for anatase and rutile TiO ₂ by different doping modes based on GCA + U calculations. RSC Advances, 2014, 4, 32100.	1.7	22
46	Activate metallic copper as high-capacity cathode for lithium-ion batteries via nanocomposite technology. Nano Energy, 2018, 54, 59-65.	8.2	22
47	Incorporating <i>p</i> â€Phenylene as an Electronâ€Donating Group into Graphitic Carbon Nitride for Efficient Charge Separation. ChemSusChem, 2019, 12, 4285-4292.	3.6	22
48	Morphology-dependent formaldehyde detection of porous copper oxide hierarchical microspheres at near-room temperature. Microporous and Mesoporous Materials, 2020, 302, 110232.	2.2	22
49	Influence of carbon and yttrium co-doping on the photocatalytic activity of mixed phase TiO 2. Chinese Journal of Catalysis, 2017, 38, 1688-1696.	6.9	21
50	Insights into synergistic effect of Pd single atoms and sub-nanoclusters on TiO2 for enhanced photocatalytic H2 evolution. Chemical Engineering Journal, 2022, 450, 137873.	6.6	21
51	High Methanol Gas-Sensing Performance of Sm2O3/ZnO/SmFeO3 Microspheres Synthesized Via a Hydrothermal Method. Nanoscale Research Letters, 2019, 14, 57.	3.1	20
52	Porous Anatase TiO ₂ Nanocrystal Derived from the Metal–Organic Framework as Electron Transport Material for Carbon-Based Perovskite Solar Cells. ACS Applied Energy Materials, 2020, 3, 6180-6187.	2.5	20
53	Mechanistic insight into the dispersion behavior of single platinum atom on monolayer g-C3N4 in single-atom catalysts from density functional theory calculations. Applied Surface Science, 2021, 566, 150697.	3.1	19
54	Design of ultrasensitive Ag-LaFeO3 methanol gas sensor based on quasi molecular imprinting technology. Scientific Reports, 2018, 8, 14220.	1.6	18

#	Article	IF	CITATIONS
55	Nanoporous Carbon Derived from Green Material by an Ordered Activation Method and Its High Capacitance for Energy Storage. Nanomaterials, 2020, 10, 1058.	1.9	18
56	Microwave-assisted synthesis of porous and hollow <i>α</i> -Fe ₂ O ₃ /LaFeO ₃ nanostructures for acetone gas sensing as well as photocatalytic degradation of methylene blue. Nanotechnology, 2020, 31, 215601.	1.3	17
57	Constructing hierarchical SnO2 nanoflowers for enhanced formaldehyde sensing performances. Materials Letters, 2020, 263, 126843.	1.3	16
58	A double perovskite LaFe1-xSnxO3 nanocomposite modified by Ag for fast and accurate methanol detection. Materials Research Bulletin, 2020, 132, 111006.	2.7	15
59	Enhanced performance of an acetone gas sensor based on Ag-LaFeO ₃ molecular imprinted polymers and carbon nanotubes composite. Nanotechnology, 2020, 31, 405701.	1.3	14
60	Methanol Gas-Sensing Properties of SWCNT-MIP Composites. Nanoscale Research Letters, 2016, 11, 522.	3.1	12
61	Carbonâ€Based Printable Perovskite Solar Cells with a Mesoporous TiO ₂ Electron Transporting Layer Derived from Metal–Organic Framework NH ₂ â€MILâ€125. Energy Technology, 2021, 9, 2000957.	1.8	11
62	Ultrasensitive ppb-level trimethylamine gas sensor based on p–n heterojunction of Co ₃ O ₄ /WO ₃ . Nanotechnology, 2021, 32, 505511.	1.3	11
63	Type II heterojunction promotes photoinduced effects of TiO ₂ for enhancing photocatalytic performance. Journal of Materials Chemistry C, 2022, 10, 6341-6347.	2.7	11
64	Impact of sulfur-, tantalum-, or co-doping on the electronic structure of anatase titanium dioxide: A systematic density functional theory investigation. Materials Science in Semiconductor Processing, 2015, 33, 94-102.	1.9	10
65	Ag-LaFeO3 nanoparticles using molecular imprinting technique for selective detection of xylene. Materials Research Bulletin, 2018, 107, 271-279.	2.7	10
66	Efficient Bifacial Passivation Enables Printable Mesoscopic Perovskite Solar Cells with Improved Photovoltage and Fill Factor. Solar Rrl, 2020, 4, 2000288.	3.1	10
67	Formation of Multiphase Soft Metal from Compositing GaInSn and BiInSn Alloy Systems. ACS Applied Electronic Materials, 2022, 4, 112-123.	2.0	10
68	The recent research progress and application of nanoparticles and ions supporting by covalent organic frameworks. Microporous and Mesoporous Materials, 2022, 335, 111701.	2.2	10
69	Structural and electronic properties of Cu ₂ Q and CuQ (Q = O, S, Se, and Te) studied by first-principles calculations. Materials Research Express, 2018, 5, 016305.	0.8	9
70	Hybrid cobalt–manganese oxides prepared by ordered steps with a ternary nanosheet structure and its high performance as a binder-free electrode for energy storage. Nanoscale, 2021, 13, 2573-2584.	2.8	8
71	Silver nanoparticles embedded 2D g-C ₃ N ₄ nanosheets toward excellent photocatalytic hydrogen evolution under visible light. Nanotechnology, 2022, 33, 175401.	1.3	8
72	The janus in monodispersed catalysts: synergetic interactions. Journal of Materials Chemistry A, 2021, 9, 5276-5295.	5.2	7

#	Article	IF	CITATIONS
73	Rice-grain Sm2O3/SmFeO3 nanoparticles as high selectivity formaldehyde gas sensor prepared by precipitation. Materials Letters, 2021, 292, 129416.	1.3	7
74	Highly enhanced photocatalytic hydrogen evolution activity by modifying the surface of TiO ₂ nanoparticles with a high proportion of single Cu atoms. Catalysis Science and Technology, 2022, 12, 3856-3862.	2.1	7
75	In2O3 Hollow porous nanospheres loaded with Ag nanoparticles to achieve wide concentration range triethylamine detection. Materials Research Bulletin, 2022, 153, 111881.	2.7	7
76	Pompon-like MnO2 and N/O doped nanoporous carbon composites with an ultrahigh capacity for energy storage. Electrochimica Acta, 2020, 363, 137240.	2.6	6
77	Mechanism of the Dimethylammonium Cation in Hybrid Perovskites for Enhanced Performance and Stability of Printable Perovskite Solar Cells. Solar Rrl, 2022, 6, 2100923.	3.1	6
78	Synergistic effects of nonmetal co-doping with sulfur in anatase TiO ₂ : a DFT + U study. Physical Chemistry Chemical Physics, 2015, 17, 3426-3434.	1.3	5
79	Anatase Mg0.05Ta0.95O1.15N0.85: a novel photocatalyst for solar hydrogen production. RSC Advances, 2016, 6, 86240-86244.	1.7	5
80	Structural and electronic properties of low-index stoichiometric Cu2ZnSnS4 surfaces. Materials Research Express, 2018, 5, 055902.	0.8	4
81	Theoretical study of CO oxidation on Au1/Co3O4 (110) single atom catalyst using density functional theory calculations. Materials Science in Semiconductor Processing, 2021, 123, 105578.	1.9	4
82	Unique and Excellent Paintable Liquid Metal for Fluorescent Displays. ACS Applied Materials & Interfaces, 2022, 14, 23951-23963.	4.0	4
83	High response and selective ag-SmFeO <inf>3</inf> methanol gas sensors. , 2017, , .		3
84	A Bidirectional Nanomodification Approach for Synthesizing Hierarchically Architected Mixed Oxide Electrodes for Oxygen Evolution. Small, 2021, 17, e2007287.	5.2	3
85	Synthesis of photocatalytic TiO2 nanoparticles at low cost. Transactions of Nonferrous Metals Society of China, 2006, 16, s411-s413.	1.7	2
86	Antibiotic properties of Al2O3 doping silver. Central South University, 2005, 12, 263-265.	0.5	1
87	A SIMPLE ROUTE FOR SYNTHESIS OF TIN DIOXIDE NANORODS BASED ON IMPROVED SOLID-STATE REACTIONS. , 2011, , .		1
88	Preparation and Characterization of TiO2-Hybrid SiO2 Porous Film. , 2009, , .		0
89	Fabrication of low operating temperature acetone sensor based on ag-lafeo <inf>3</inf> nanomaterials. , 2017, , .		0